Communications in Computational Chemistry
Commun. Comput. Chem. Vol. 8, No. 1, 12-24
doi: 10.4208/cicc.2025.284.01
Regular Article

Optical Field Control of Ultrafast Dynamics in Complex Systems: Frontiers and Perspectives

Luxiang Zhu[1], Haoyang Xu[1], Lei Niu[2] and Jin Wen[1,*]

[1]*State Key Laboratory of Advanced Fiber Materials, College of Materials Science and Engineering, Donghua University, Shanghai 201620, China;*

[2]*School of Mathematics and Statistics, Donghua University, Shanghai 201620, China.*

[*] Corresponding authors: jinwen@dhu.edu.cn.

Received 11 Oct. 2025; Accepted (in revised version) 4 Dec. 2025

Abstract: Ultrafast optical field control has progressed from merely observing photochemical dynamics to actively steering molecular transformations. However, a persistent gap between theory and experiment continues to impede predictive control in complex systems. Femtosecond and attosecond techniques now allow real-time manipulation of electronic evolution, vibrational motions, and bond dissociation in small molecules. However, these achievements often fail to translate to condensed-phase environments due to increasing molecular complexity, environmental decoherence, and stringent instrumental constraints. This review summarizes recent advances in which pump-probe experiments — utilizing tailored pulse parameters such as intensity, wavelength, phase, and polarization — have uncovered key control mechanisms while also revealing critical challenges in scalability and reproducibility. Theoretical progress in quantum control methods (e.g., local control theory) and mixed quantum-classical simulations has clarified fundamental principles, yet often remains disconnected from experimental implementation. We propose that machine learning (ML) serves as an essential bridge to close this gap. By constructing hybrid theory-experiment databases and training environment-aware models, ML can capture complex pulse-branching correlations and system-environment couplings. These models effectively translate theoretical insights into experimentally feasible pulse designs, thereby paving the way for designing light-driven molecular processes that extend beyond gas-phase paradigms to functional materials.

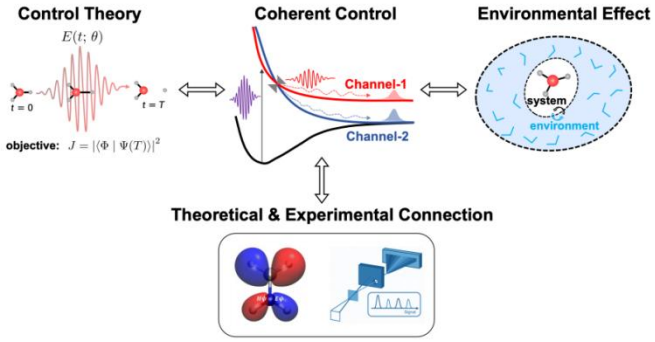

Key words: optical field control, pump-probe spectroscopy, coherent control, nonadiabatic dynamics.

1. Introduction

Ultrafast laser technologies have transformed photochemistry from passive observation to active control, meaning the deliberate shaping of laser pulses to influence reaction pathways, evolving from 1970s isotope separation to 1980s quantum pathway manipulation [1-3]. The 1990s breakthrough of femtosecond pump probe techniques enabled direct imaging of transition states, earning the 1999 Nobel Prize and establishing light-driven control as a cornerstone of modern physical chemistry [4]. Today, femtosecond and attosecond pulses steer electronic and nuclear dynamics at natural timescales, positioning ultrafast photochemistry at the forefront of atomic-scale molecular engineering [5-7].

A few systems have successfully demonstrated coherent control of phenomena such as electronic relaxation and bond dissociation in the gas phase. However, this very success also reveals a critical limitation: experimental control remains system-specific due to incomplete knowledge of high-dimensional potential energy surfaces (PESs) [8,9]. Early studies proved the concept but exposed a fundamental gap between theoretical principles and experimental generalizability, driving advances in quantum dynamics that now enable rational pulse design [10]. As the field expands to larger π-conjugated and biologically relevant systems, novel light sources offer unprecedented manipulation opportunities [11]. Yet dense electronic manifolds, environmental decoherence, and condensed-phase pulse distortions impede robust control, highlighting the persistent theory-experiment disconnect [12]. Prior reviews have effectively summarized experimental strategies and applications in photochemical control [13,14], but a systematic analysis of molecular dynamics-a critical perspective for predictive control-has remained relatively limited.

We bridge this divide by organizing the review around dynamical processes rather than control methods alone. Tracing the transition from gas-phase to condensed-phase systems, we show how theory must evolve to address environmental complexity. Crucially, we advance emerging frontiers like machine learning-assisted pulse optimization and environment-aware modeling to demonstrate how theory now guides experimental design. By synthesizing these advances, we establish a predictive framework for optical field control in complex systems — moving beyond cataloging phenomena to actionable control pathways. The remainder of this review is organized as follows. Section 2 surveys key experimental advances in optical-field-controlled molecular dynamics. Section 3 introduces the corresponding theoretical frameworks that simulate these processes and elucidate the underlying mechanisms. Section 4 discusses emerging machine-learning strategies that connect theoretical insight with experimental constraints to enable scalable optical field control.

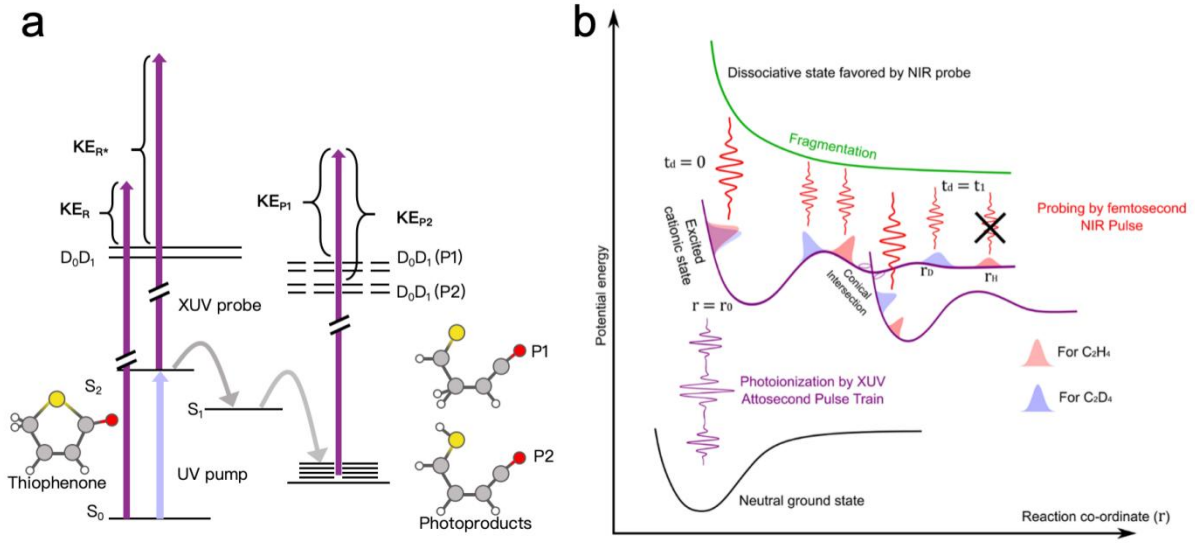

Figure 1. (a) UV pump and XUV probe tracking the ring-opening dynamics of thiophenone, showing relaxation via $S_2 \rightarrow S_1 \rightarrow S_0$ and subsequent formation of open-chain photoproducts (ref [15]). (b) Attosecond XUV pump-NIR probe experiment on ethylene isotopologues, revealing isotope-dependent relaxation dynamics. Adapted with permission from ref [16]. *Copyright © 2022, American Chemical Society.*

2. Coherent control of photochemical reactions

2.1 Pump-probe studies in small molecules

Small molecular systems, such as IBr, CH_4, C_2H_4, and CH_3I, serve as ideal models for validating laser field control strategies, owing to their well-defined electronic structures and low-dimensional PESs. These systems provide a foundational platform for elucidating fundamental photophysical and photochemical processes, including electronic relaxation, nonadiabatic transitions, and bond-selective dissociation, showing direct insights into ultrafast reaction dynamics under tailored optical fields [17]. In recent years, advances have transformed theoretical principles into experimental reality. For instance, Wei et al. observed large-amplitude vibrational wave packets and dissociative ionization in strong-field ionized CH_2I_2, revealing nonadiabatic dynamics under intense laser excitation [18]. Ridente et al. employed femtosecond X-ray free-electron lasers to track symmetry breaking and coherent relaxation in the CH_4^+ cation in real time [19]. Additionally, González-Vázquez et al. combined synchrotron radiation with double imaging photoelectron photoion coincidence spectroscopy techniques to capture the conical intersection involved in the internal conversion of CH_3I^+ [20]. Together, these studies confirm that small molecules exhibit rich ultrafast dynamics and demonstrate the critical role of advanced light sources in probing and controlling photochemical pathways.

Building on this foundation, we highlight several representative pump-probe studies that exemplify how advanced light sources bridge molecular dynamics and control theory. As shown in **Figure 1a**, Pathak et al. used a ultraviolet/extreme ultraviolet (UV/XUV) experiment in gas-phase thiophenone, where a 265 nm pump initiated S_2 excitation and a 19.24 eV XUV free-electron laser probe tracked ultrafast ring opening via time-resolved photoelectron spectroscopy [15]. The resulting spectra reveal a C-S elongation and ring opening within $\lesssim$ 350 fs through the $S_2 \rightarrow S_1 \rightarrow S_0$ nonadiabatic pathway, followed by isomer interconversion and delayed fragmentation on vibrationally hot S_0 (10-600 ps). Critically, this trajectory — which maps directly onto a conical intersection—provides direct experimental validation of theoretical predictions for nonadiabatic reaction pathways. Beyond these femtosecond pump-probe experiments, attosecond-resolved studies further extend ultrafast spectroscopy into the electronic timescale. Representative examples include attosecond high-harmonic charge-migration spectroscopy in N_2/CO_2, chiroptical measurements of methyloxirane, and vibrationally resolved reconstruction of attosecond beating by interference of two-photon transitions (RABBIT) delays in CO_2 [21-23]. Collectively, these studies show that attosecond spectroscopy can quantify electronic, chiral, and mode-specific electron-nuclear dynamics on their natural timescales. As another example, **Figure 1b** highlights an approach of attosecond XUV pump with an NIR probe by Vacher et al., where an at tosecond XUV pulse pumped ethylene cations to multiple excited states, while a near-infrared (NIR) probe resolved few-femtosecond nuclear dynamics and electron-nuclear coupling [16]. By comparing protiated and deuterated isotopologues, the study established the first experimental benchmark for electronic-timescale isotope effects — a key test for quantum dynamics

simulations. These advances demonstrate how ultrafast spectroscopy effectively bridges theoretical models and experimental observations by providing quantifiable, time-resolved dynamical data, thereby establishing a predictive control framework essential to modern photochemistry.

The advancement from femtosecond to attosecond temporal resolution has opened the door to directly observing electronic dynamics, thereby elevating pump-probe studies from analytical tools into potential platforms for active control. Although current attosecond experiments primarily map dynamical processes, their methodological breakthroughs—particularly the direct observation of electron-nuclear coupling — have expanded experimental capabilities. These advances pave the way for future coherent manipulation, meaning phase-controlled steering of electronic-scale dynamics [24]. Critically, such work not only elucidates nonadiabatic mechanisms in small-molecule systems but also establishes the experimental foundation needed to design laser-driven control of reaction pathways, effectively bridging theoretical models with real-world photochemical engineering.

2.2 Coherence control in small molecules

This synergy between temporal resolution and control is demonstrated through pump-probe spectroscopy, which has emerged as the central technique for femtosecond-resolved state-to-state dynamics [25]. Its full potential is realized when integrated with coherent control strategies that actively manipulate reaction pathways. By tuning key pulse parameters—such as ellipticity to steer dissociation channels, phase modulation for interference-based selectivity, and polarization shaping to direct ionization—researchers achieve unprecedented control over molecular outcomes [26-28]. This parametric tunability is exemplified across diverse systems: for instance, Corrales et al. controlled fragment angular distributions in CH_3I photodissociation via strong field [29], while Kaufman et al. manipulated internal conversion in ionized molecules [27]. Similarly, Varvarezos et al. demonstrated wavelength-dependent channel branching in methane [30], and Ridente et al. captured symmetry breaking in CH_4^+ within 50 fs using X-ray probes [19].

The strategic role of laser parameters is further illuminated in **Figure 2a**, where Basnayake et al. under strong-field conditions (800 nm and ≈ 35fs), the branching ratios of all dissociation channels of the ethane dication—produced via strong-field double ionization—were measured using ion–ion three-dimensional coincidence momentum imaging [26]. The study revealed that these branching ratios can be effectively controlled by varying the laser pulse ellipticity, scanned from near-linear to highly elliptical (approximately e = 0.05-0.85). Specifically, the relative yield of the two-body channel ($CH_3^+ + CH_3^+$) peaks near $e \approx 0.6$, while channels involving H^+ are minimized around the same ellipticity. Meanwhile, the relative fraction of three-body channels also varies systematically with ellipticity, demonstrating clear experimental controllability over selective dissociation pathways [26].

As depicted in **Figure 2b**, Zhou et al. used a pump-probe reaction microscope with ultrashort laser pulses to directly observe and characterize the ultrafast dynamics of D_3^+ formation from the gas-phase D_2−D_2 dimer [31]. In their experiment, single-color 790 nm pulses were first used to distinguish two distinct formation pathways: a rapid double-ionization channel occurring within the pump pulse duration (within 35 fs), and a slower single-ionization channel with a formation time ~ 139 fs. Subsequently, a two-color pump scheme with phase scanning was applied to achieve controlled modulation of the D_3^+ formation direction. The high-momentum branch exhibited sinusoidal asymmetry as a function of the phase, whereas the low-momentum branch remained largely unresponsive—indicating that the two-color femtosecond field can selectively steer the product formation in this bimolecular reaction. Collectively, these studies establish a unified principle: laser field parameters (intensity, wavelength, ellipticity, and phase) are not mere observational tools but active control knobs for product distribution, directionality, and channel branching. In small molecules—from halomethanes to hydrocarbons—this parametric precision has resolved nonadiabatic dynamics, electron-nuclear coupling, and dissociation pathways. Critically, the ability to rationally design light fields for specific outcomes provides the essential experimental foundation for scaling control to complex systems, transforming photochemistry from observation to engineering.

2.3 Pulse-driven control in complex systems

As optical field control advances from small molecules to complex systems, the increased density of electronic states and strong vibrational couplings in π-conjugated molecules and photosensitive proteins present formidable challenges for selective manipulation [32]. Yet recent breakthroughs demonstrate that vibrationally selective control remains achievable in condensed phases, but by strategically leveraging molecular design and spectroscopic insight to turn environmental complexity into a controllable parameter. We will discuss the experimental progress in three aspects: direct light-induced charge transfer, molecular-design-enabled control, environment-coupled reaction dynamics.

Direct light-induced charge transfer. This paradigm shift is exemplified by Delor et al.'s work on Pt(II)-acetylide assemblies [33,34]. In their 2015 study, they utilized ultraviolet pump pulses to excite charge-transfer states and combined mid-infrared pulses to selectively excite C≡C bridge vibrations, thereby effectively modulating the dynamics of light-induced electron transfer [33]. The experimental results clearly showed that this targeted vibrational excitation could both promote and suppress charge transfer, and in some cases, the suppression efficiency could approach 100% [33]. Building on this approach shown in **Figure 3**, Delor et al. further designed a "fork" system (^{12}C isotopic substitution on one acetylide bridge), creating two electron-transfer pathways with distinct vibrational properties [34]. Critically, multi-pulse UV-IR sequences achieved spatial pathway selection—suppressing transfer along the excited bridge while promoting the alternative route—providing the first experimental validation of vibronic design principles for directional control in solution.

Molecular-design-enabled control. Beyond direct field control, an alternative strategy combining spectroscopic diagnostics with molecular design has also recently emerged. Paulus and colleagues identified key modes (Fe-N stretch and ligand torsion) governing metal-ligand charge transfer (MLCT) decay, by mapping vibronic coherences in Fe(II) polypyridyl complexes [35]. Based on these observations, they synthetically modified the ligand backbone by introducing Cu^+ ions to restrict these specific vibrational degrees of freedom. The results were encouraging: the lifetime of the redesigned complex's MLCT state was extended by more than 20 times (from approximately 110 fs to 2.6 ps) [35]. This study strongly demonstrated how ultrafast diagnostics can directly inform molecular design to overcome environmental decoherence.

In the field of biological macromolecules, Hutchison and colleagues achieved direct optical control of chromophore photoisomerization in the reversibly photoswitchable fluorescent protein by combining femtosecond pump-probe time-resolved serial femtosecond crystallography with two-color two-pulse coherent control technology, as shown in **Figure 4a**. Under standard 400 nm pump-X-ray probe conditions (spatial resolution 1.35 Å, 50-fs-wide bins), they resolved sub-angstrom nuclear motions and hydrogen bond rearrangements at the active site [36]. When a two-color pump-dump-probe scheme was introduced (400 nm pump + 515 nm dump, 350 femtosecond delay), the X-ray difference electron density was significantly enhanced, while the excited-state signal and photoisomerization yield were completely suppressed; if the dump delay was increased to approximately 2 ps (beyond the vibrational dephasing time), this amplification effect disappeared [36]. These results identified ground-state vibrations as the origin of early nuclear motions, providing a verified optical control mechanism for macromolecules.

Environment-coupled reaction dynamics. Further delving into the mechanisms of microscopic chemical reaction dynamics, Rana et al. demonstrated optical field control in microsolvated 4-aminobenzoic acid protonated ion ($4ABAH^+(H_2O)_6$) clusters (**Figure 4b**) [37]. They prepared cold clusters in an ion trap at 6K and employed an isomer-selective IR pump/UV probe scheme. By selectively exciting the ν_{bOH} (3290 cm^{-1}) of the O-isomer or the ν_{bNH} (3110 cm^{-1}) of the N-isomer, they were able to directionally trigger proton migration along the microsolvated water bridge and monitor the subsequent population evolution via UV probe. The time-resolved signal showed a mono-exponential decay: the decay constant for O → N was 2.1 ± 0.1 μs, while the rise constant for N → O was 1.3 ± 0.1 μs; at higher initial internal energy (e.g., N-isomer excited at 3645 cm^{-1}), the rate accelerated to 0.9 μs [37]. This closed-system demonstration—where theory can precisely model energy-defined dynamics—provides the critical bridge from idealized gas-phase studies to complex, environmentally coupled systems.

These advances show a unifying principle: controlling complex systems lies not in overcoming environmental interactions, but in harnessing them through spectroscopically informed molecular design—thereby transforming complexity from a barrier into a control parameter.

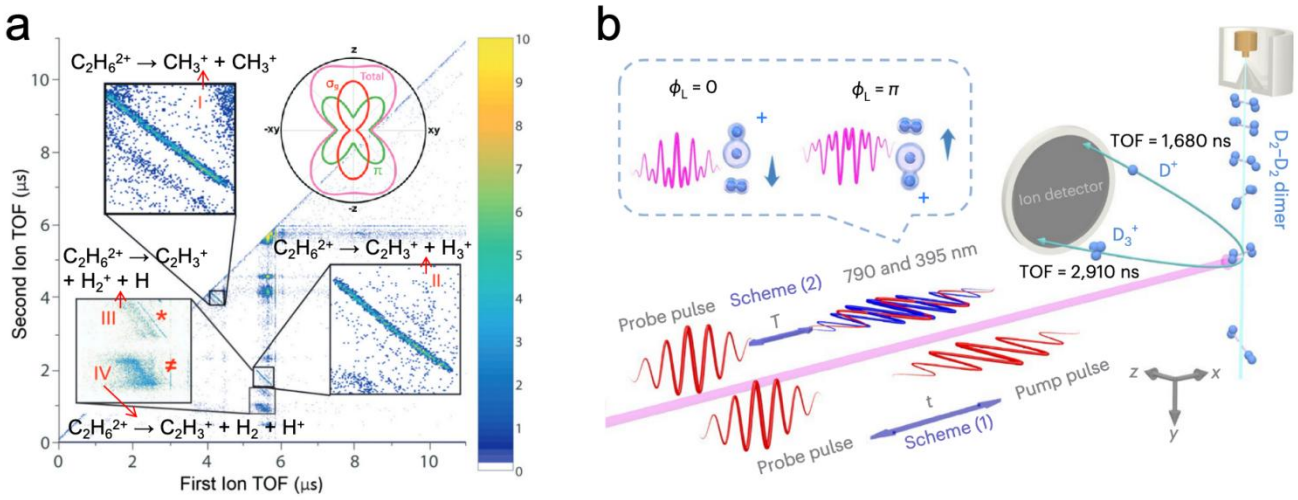

Figure 2. (a) Coincidence ion-ion momentum maps for ethane dissociative double ionization under strong fields; the inset shows the orbital contributions (σ_g and π) to the total ionization yield, with regions III and IV marking distinct fragmentation pathways. Adapted with permission from ref [26]. *Copyright © 2021, Royal Society of Chemistry.* (b) Two-color femtosecond laser scheme driving D_3^+ formation from D_2-D_2 dimers, with relative phase control over fragment emission directionality. Adapted from ref [31]. First published in Nature Chemistry by Springer Nature. © 2023.

2.4 Challenges in controlling complex systems

Despite successful demonstrations of optical coherent control in complex systems [33–36], significant experimental challenges persist in advancing laser-field control methodologies [12]. The transition from studying small molecules to manipulating larger, more complex systems exposes fundamental limitations that currently constrain practical applications.

A primary challenge stems from the increased density of states and intensified vibronic couplings in larger molecular systems. These factors drastically shorten coherence lifetimes and diminish the selectivity of intended reaction pathways. For instance, a 2017 study on rhodopsin-like proteins demonstrated that phase-shaped laser pulses failed to control the photoisomerization process under single-photon conditions [12]. The experiments revealed that phase modulation produced no consistent or reproducible effect on the final isomerization yield in weak-field regimes, which aligns with theoretical predictions that strong electronic decoherence—occurring within tens of femtoseconds in room-temperature condensed phases—rapidly erases coherent effects, thereby nullifying single-photon coherent control strategies [12].

Instrumentation requirements present another major hurdle. Achieving theoretically optimal conditions demands extreme stability in pulse duration, phase, and polarization, which is experimentally non-trivial. As seen in Hutchison's work, precisely timed, phase-stable two-color pulses were essential for excited-state depletion prior to decoherence [36]. Similarly, control schemes that modulate branching ratios via laser ellipticity require exceptionally stable ellipticity and intensity to be effective [26]. These technical demands highlight the stringent parameter windows within which coherent control must operate.

Environmental effects in condensed phases or at interfaces further weaken coherence. Factors such as rapid energy dissipation, orientational averaging, and inhomogeneous broadening compress the controllable time window and weaken phase-dependent signatures. This explains why many high-fidelity control and diagnostic demonstrations, such as those by Vacher et al. and Pathak et al., have been conducted in gas phases or molecular beams, where environmental decoherence is minimized [15,16].

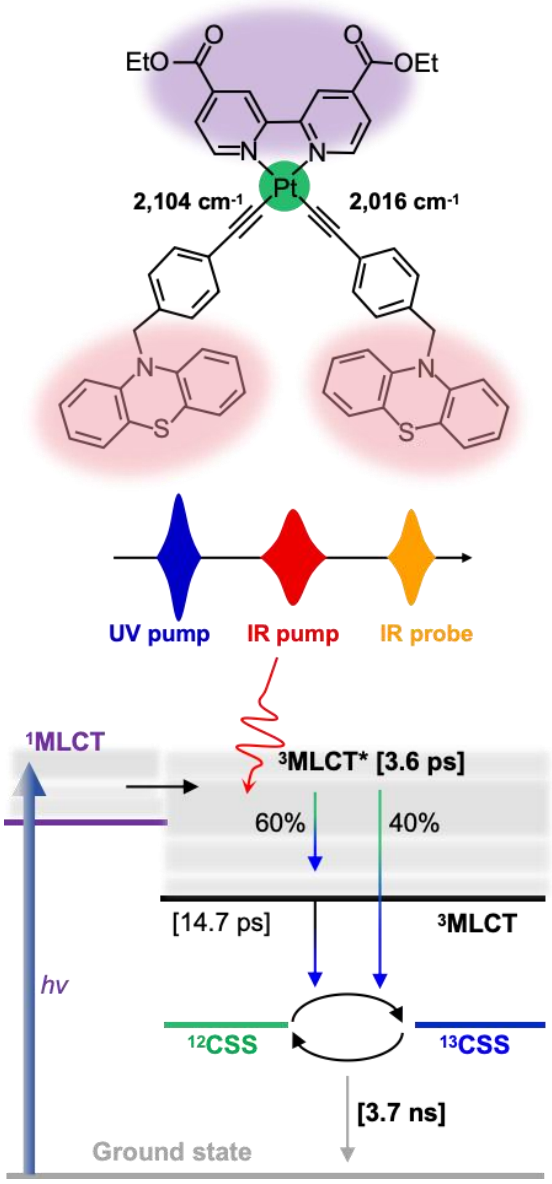

Figure 3. In an isotopically differentiated two-bridge "molecular fork", a narrowband mid-IR pulse selectively excites a bridge C≡C stretch to bias ^{3}MLCT* → charge-separated state (CSS) branching within a picosecond window (UV pump-IR pump-IR probe) (ref [34]).

In summary, while current studies provide a clear time-resolved picture for small molecules and select complex systems, observables remain largely confined to product distributions or aggregate time-resolved signals [17]. Under strong environmental coupling and hardware constraints, the coherence window is short and channel assignment is often confounded. Realizable field shapes are restricted, leaving a substantial gap between merely observing ("seeing") and actively manipulating ("controlling") quantum dynamics. Bridging this gap requires anchoring theory to experimentally accessible signals, delineating the effective coherence window, identifying dominant couplings and branching mechanisms, and mapping these insights onto experimentally feasible pulse parameters to generate testable predictions [14,38].

3. Dynamical control theory

3.1 Quantum control theory

Despite substantial progress in resolving ultrafast dynamics, observable signals alone remain insufficient to reveal the mechanisms of optical field control. While experimental advances have demonstrated the feasibility of optical field control in increasingly complex molecular systems [39,40], a fundamental understanding of how shaped light fields direct reaction pathways requires insights from quantum dynamics. Theoretical studies of coherent control have thus been essential to elucidate the underlying mechanisms by which tailored laser pulses steer molecular dynamics at the quantum level. In this context, quantum dynamical (QD) simulations on prototypical systems provide critical benchmarks for testing pulse designs and dissecting molecular dynamical processes [17,41]. A widely adopted starting point for such theoretical investigations is a two-state model representing the light-matter interaction [10]. Within this framework, the ground- and excited-state Born-Oppenheimer PESs are coupled via the radiation field through the transition dipole operator, enabling a quantitative description of control phenomena such as population transfer and wavepacket interference [42]. The Hamiltonian can be written as a 2 × 2 operator matrix,

$$H = \begin{pmatrix} H_a & \mu E(t) \\ \mu E(t) & H_b \end{pmatrix}, \quad (1)$$

where H_a and H_b are the nuclear Hamiltonians associated with the ground and excited electronic states, respectively, and μ denotes the transition dipole moment. The corresponding time-dependent Schrödinger equation (TDSE) is expressed as

$$i\hbar \frac{\partial}{\partial t}\begin{pmatrix} \psi_a \\ \psi_b \end{pmatrix} = \begin{pmatrix} H_a & \mu E(t) \\ \mu E(t) & H_b \end{pmatrix}\begin{pmatrix} \psi_a \\ \psi_b \end{pmatrix}. \quad (2)$$

Within this framework, the system is initialized in the vibrational ground state of the lower electronic surface, expressed as $\psi_a = \psi_0$ with $H_a\psi_0 = E_a\psi_0$. Upon application of the external field $E(t)$, the off-diagonal coupling terms, $\mu E(t)$, drive population transfer between the two states. Importantly, the temporal profile of $E(t)$—including its amplitude, phase, duration, and interpulse delay—directly modulates the coherence established between ψ_a and ψ_b, thereby steering quantum interference among competing transition pathways. In this manner, the Hamiltonian formulation furnishes the theoretical basis for coherent control over photochemical dynamics [43].

Building on this theoretical foundation, QD simulations have served as essential benchmarks, illustrating how specific pulse sequences realize such control in practice. These case studies effectively translate the abstract Hamiltonian picture into concrete dynamical scenarios, demonstrating how the interplay of pulse delay, chirp, and polarization governs state-to-state outcomes—a connection most clearly revealed in pump-probe and pump-dump control schemes, which we will discuss below.

Pump-probe/pump-dump control. Representative quantum-dynamics simulations illustrate how tailored pulse sequences enable coherent control of excited-state dynamics through distinct field configurations. In the pump-probe scheme (**Figure 5a**), an intense IR pump pulse first launches a nuclear wave packet along a bending or stretching mode on an excited potential-energy surface. A delayed UV probe pulse then promotes the evolving wave packet to higher electronic states, leading to dissociation [44]. Quantum-dynamical analyses reveal two characteristic control mechanisms: the formation of transient light-induced potentials ("photon locking"), where resonant coupling between adjacent states creates dynamic barriers that temporarily trap or reflect the wave packet; and selective amplitude depletion ("hole burning") at the leading or trailing edge of the wave packet, which reshapes its spatial distribution and phase [44]. These effects demonstrate how field timing and frequency modulation can redirect molecular motion on femtosecond timescales, thereby altering branching ratios among competing reaction channels.

A complementary strategy is realized in the pump-dump scheme (**Figure 5b**), where a sequence of excitation and de-excitation pulses orchestrates population transfer between ground and excited states. For example, in simulations of photoisomerization in H_2POSD, a resonant pump pulse drives the molecule from the ground state to a repulsive excited surface, initiating rotation around a stereogenic bond [45]. A subsequent dump pulse, applied at a precisely tuned delay, projects the wave packet back to the ground-state minimum corresponding to the target enantiomer before dissociation occurs. By varying the interpulse delay and phase, the relative yield of L- and R-configurations can be selectively enhanced or even inverted, achieving coherent discrimination between competing pathways [45]. Together, the pump-probe and pump-dump paradigms demonstrate how femtosecond pulse sequences manipulate wave-packet evolution on coupled PESs, establishing the mechanistic basis for modern optimal-control strategies.

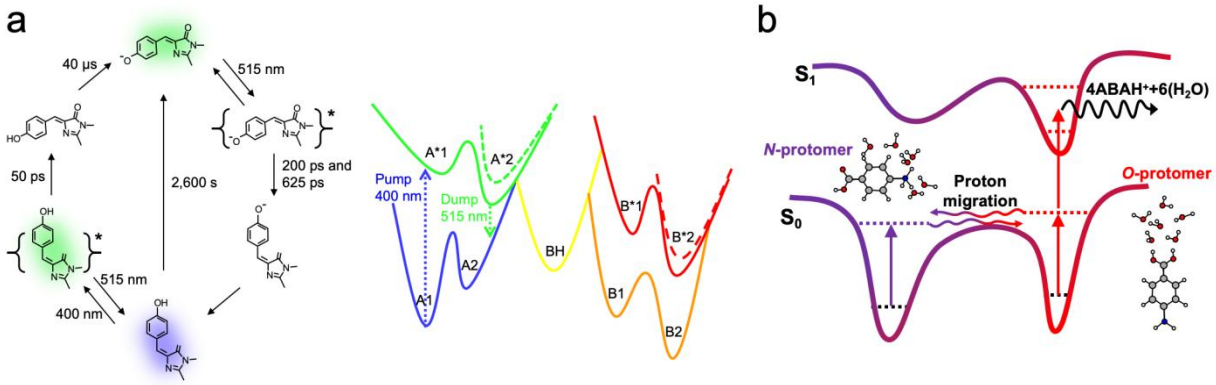

Figure 4. (a) A two-color pump-dump-probe scheme amplifies ground-state vibrational coherence, distinguishing coherent vibrational motions in the isomerization process (ref [36]). (b) In the cold cluster $4ABAH^{+}\cdot(H_2O)_6$, a protomer-selective IR-pump/UV-probe approach is employed to trace water-mediated proton migration on the microsecond timescale (ref [37]).

Combination with IR and UV. Beyond purely electronic excitation, coherent control can also exploit vibronic coupling to achieve selective molecular manipulation. A representative example, illustrated in **Figure 6a**, involves polarization-sensitive excitation in which an IR pulse drives a torsional vibration whose transition-dipole orientation differs between mirror-image configurations [46]. This results in preferential population transfer in one enantiomer, generating a transient nuclear bias that a subsequent UV pulse converts into asymmetric dissociation or photoactivation. This mechanism demonstrates how vibrational prealignment can break symmetry equivalence and enable enantioselective photochemistry through coupled nuclear and electronic motion.

A complementary strategy, depicted in **Figure 6b**, highlights the cooperative role of sequential IR-UV excitation in steering nuclear wave-packet dynamics [47]. Here, the IR pulse deposits energy along a specific vibrational coordinate, creating a non-equilibrium distribution on the ground-state surface, while the delayed UV pulse promotes this biased ensemble into multiple excited-state channels. By tuning the relative phase, delay, or polarization between the two pulses, interference among competing excitation pathways can be adjusted to favor specific product branches or chiral outcomes [47]. Reversing the IR polarization inverts the asymmetry, confirming the coherent nature of the control process. Together, these two approaches illustrate how vibrational pre-excitation and electronic promotion can act in concert to direct chemical reactivity: the first exploits mode-specific discrimination via transition-dipole orientation, while the second achieves dynamic control through phase-coherent coupling of sequential fields. Both paradigms capture the essence of vibronic synergy as a versatile strategy for guiding molecular dynamics across complex potential-energy landscapes.

These quantum-dynamical demonstrations establish a clear mechanistic principle: pulse sequencing and shaping govern when and where a wave packet evolves on coupled PESs, while targeted vibrational preparation channels that motion into tunable reaction outcomes [48].

Theoretical frameworks for laser field design. Motivated by these insights, theoretical efforts have shifted toward systematic strategies for field design. Rather than relying on empirical pulse sequences, the control objective can be formulated as a quantum optimization problem. This shift has spurred the development of two complementary theoretical frameworks: optimal control theory (OCT) and local control theory (LCT) [49–51], which provide rigorous foundations for designing light fields that steer molecular dynamics toward desired targets.

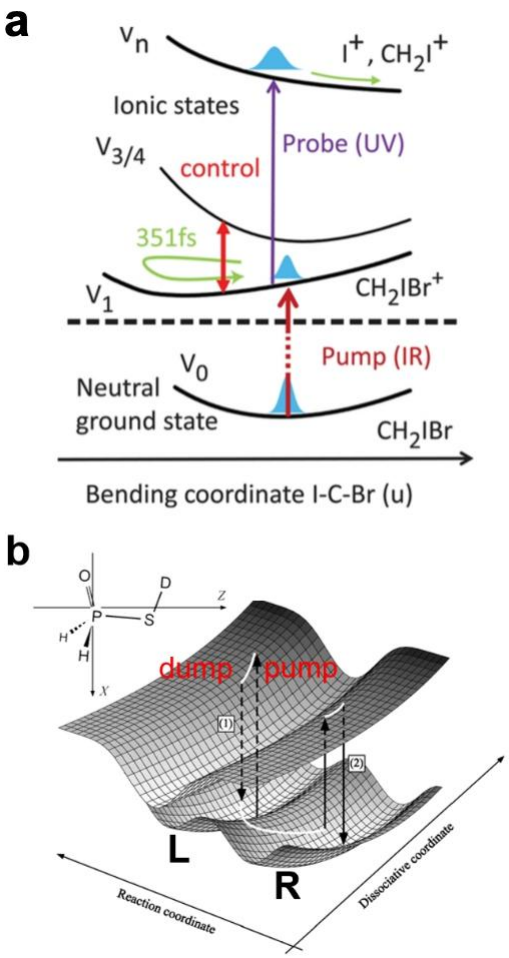

Figure 5. (a) Pump-probe sequence applied to CH_2IBr: an IR pump excites the bending coordinate, followed by a UV probe that interrogates excited-state population and controls wave packet evolution. Adapted with permission from ref [44]. *Copyright © 2012, American Chemical Society.* (b) Pump-dump strategy: wave packet propagation on coupled potential energy surfaces, where a time-delayed dump pulse transfers population toward a targeted electronic state. Adapted with permission from ref [45]. *Copyright © 2004, American Chemical Society.*

In OCT, the laser field $E(t)$ is obtained by solving a constrained variational problem [52]. A cost functional is defined as

$$J[E(t)] = \langle\psi(T)|\hat{O}|\psi(T)\rangle - \alpha\int_0^T |E(t)|^2\,dt, \qquad (3)$$

where $\hat{O}$ represents the target observable and the second term penalizes high field fluence. The optimization of J under constraint imposed by the TDSE leads to a set of coupled forward-backward propagation equations, from which an iterative update rule for the field can be derived.

$$E(t) = \frac{1}{\alpha}\,\mathrm{Im}\,\langle\chi(t)|\mu|\psi(t)\rangle, \qquad (4)$$

where $|\psi(t)\rangle$ is the propagated state and $|\chi(t)\rangle$ is the adjoint Lagrange multiplier. Since the optimization is global, OCT can design pulses that selectively enhance or suppress specific reaction pathways. For example, in quantum-dynamical simulations of uracil, OCT-generated pulses have been shown either to accelerate relaxation into the conical intersection seam or to trap population in the local S_2 minimum, effectively extending excited-state lifetimes by several picoseconds [52]. These results (illustrated in **Figure 7a**) demonstrate how OCT can reshape wave-packet evolution over multiple oscillation cycles, achieving control outcomes beyond intuitive pump-probe schemes.

In contrast, LCT constructs the control field adaptively from the instantaneous system response [50,53,54]. The objective is to enforce a monotonic increase of a target observable $J(t) = \langle\psi(t)|\hat{O}|\psi(t)\rangle$, leading to the condition

$$\dot{J}(t) = 2\,\mathrm{Im}\quad\left[\langle\psi(t)|\hat{O}\mu|\psi(t)\rangle\right]E(t) > 0. \qquad (5)$$

where λ controls the field amplitude. Unlike OCT, which relies on iterative forward-backward propagation, LCT operates in a single forward pass and adjusts dynamically to the evolving wave packet [50,53]. This makes LCT computationally efficient, though the resulting fields often exhibit complex temporal profiles that require smoothing for experimental implementation.

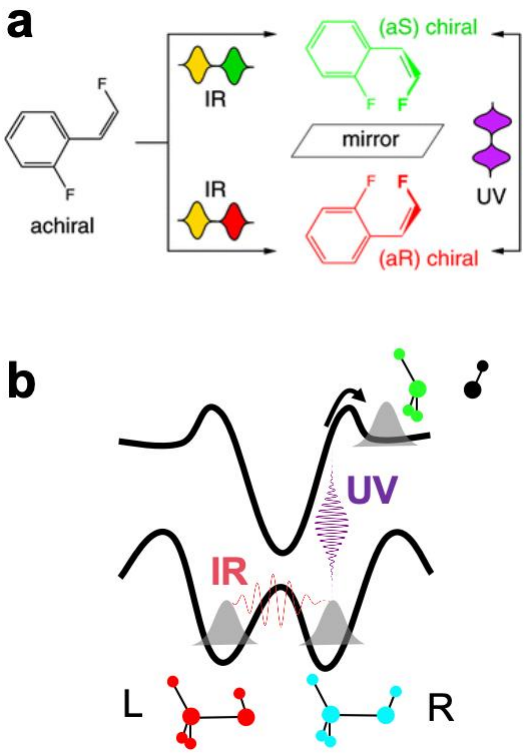

Figure 6. (a) IR-UV cooperative control of chirality: achiral precursors are converted into enantiomeric products, with field timing and sequence dictating outcome. Adapted with permission from ref [46]. *Copyright © 2007, Royal Society of Chemistry.*(b) Dual-field (IR-UV) modulation of branching: IR excitation injects vibrational energy that biases the system toward distinct reaction channels (L and R), while UV excitation promotes access to reactive excited states (ref [47]).

This inequality is satisfied by the field form

$$E(t) = \lambda\,\mathrm{Im}\quad\left[\langle\psi(t)|\hat{O}\mu|\psi(t)\rangle\right], \qquad (6)$$

Representative simulations highlight the distinct capabilities of LCT. As illustrated in **Figure 7b**, LCT can steer an initially localized wave packet across multidimensional potential-energy barriers by continuously injecting energy along the reaction coordinate [50]. In this "vibrational heating" regime, the adaptive

field responds to the instantaneous phase and direction of nuclear motion, pushing the wave packet toward the target minimum and thereby enabling processes such as isomerization or bond cleavage. The trajectory of the packet in the (Q_1, Q_2) ordinate space reveals directed motion from the reactant basin through the saddle region, into the product well-capturing the essence of field-driven barrier crossing [50].

In contrast, Marquetand et al. demonstrates the opposite regime—"vibrational cooling" or bond hardening—where the control field extracts energy from unstable modes and redistributes it into stabilizing vibrations [53]. Here, the time-dependent potential and wave-packet population map show a stepwise depletion of high-lying vibrational states within a Morse potential, accompanied by convergence toward the lowest bound level [53]. This behavior illustrates how LCT can dynamically modulate intramolecular energy flow, quenching excess vibrational energy and effectively strengthening the chemical bond.

Together, these cases underscore the dual capacity of LCT: it can either promote energy uptake to drive structural changes or facilitate energy dissipation to stabilize a reactive coordinate. In this way, OCT and LCT represent complementary control philosophies—global optimization versus instantaneous feedback—transforming pulse design from a heuristic trial-and-error process into a predictive theoretical framework that bridges quantum dynamics with experimental laser shaping [14].

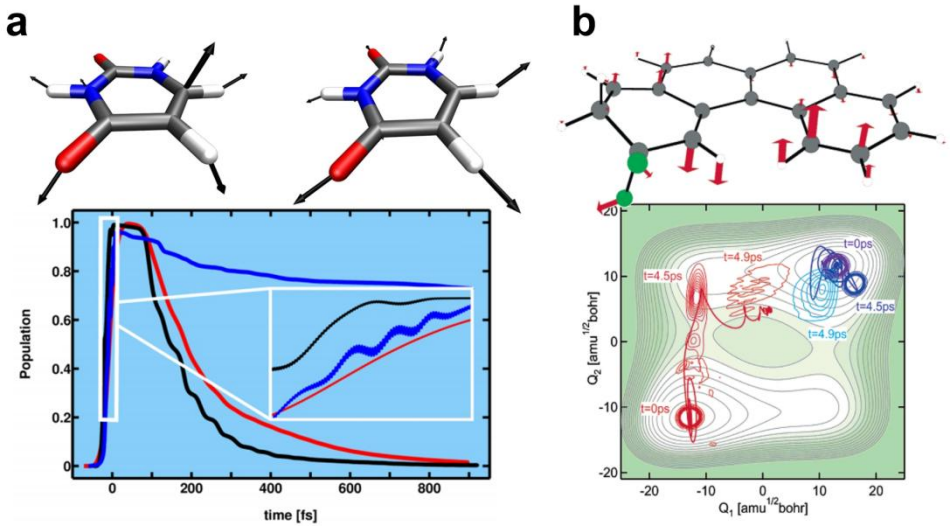

Figure 7. (a) Excited-state lifetime regulation: OCT-optimized pulses selectively extend or shorten excited-state population decay, enabling systematic control over nonadiabatic transition pathways. Adapted with permission from ref [52]. *Copyright © 2017, American Chemical Society.* (b) Barrier-crossing control: LCT directs wave packet motion along reaction coordinates, enhancing barrier surmounting and guiding wave packet through the transition-state region. Adapted with permission from ref [50]. *Copyright © 2002, American Chemical Society.*

3.2 Mixed quantum-classical simulations

Despite their successes, most OCT and LCT demonstrations have so far been confined to low-dimensional model systems, where both the potential energy landscape and wave-packet dynamics remain computationally tractable at a fully quantum-mechanical level [14]. Extending such control strategies to larger polyatomic molecules demands methodologies that can efficiently combine a quantum treatment of electronic dynamics with a classical description of nuclear motion. This need has motivated the integration of control-field design with mixed quantum–classical (MQC) methods, which offer a scalable framework for simulating laser-driven processes in chemically realistic systems [55,56].

One widely adopted approach combines local control theory with Tully's fewest-switches surface hopping (FSSH) [57,58], a method often referred to as TSH/LCT [59,60]. In this scheme, the quantum amplitudes $C_j^{(\alpha)}(t)$ for each trajectory α evolve under the time-dependent Schrodinger equation, which incorporates nonadiabatic couplings and the interaction with the external field,

$$i\hbar\dot{C}_j^{(\alpha)}(t) = \sum_i C_i^{(\alpha)}(t)[H_{ji}(R^{(\alpha)}) - i\hbar\dot{R}^{(\alpha)} \cdot d_{ji}(R^{(\alpha)}) - \mu_{ji}(R^{(\alpha)})E(t)], \quad (7)$$

where $H_{ji}(R)$ is electronic Hamiltonian matrix element, d_{ji} is the nonadiabatic coupling vector, and μ_{ji} is the transition dipoles. Within the LCT framework, the electric field is generated on-the-fly to ensure a monotonic increase in the population of a target electronic state,

$$\dot{P}_i^{(\alpha)}(t) = -\frac{2}{\hbar}E^{(\alpha)}(t)\,\mathrm{Im}\left[\sum_j C_i^{(\alpha)*}(t)\,\mu_{ij}(R^{(\alpha)})\,C_j^{(\alpha)}(t)\right], \quad (8)$$

which leads to the local control field

$$E^{(\alpha)}(t) = -\lambda\,\mathrm{Im}\left[\sum_j C_i^{(\alpha)*}(t)\,\mu_{ij}(R^{(\alpha)})\,C_j^{(\alpha)}(t)\right]. \quad (9)$$

The parameter λ controls the field amplitude. This formulation ensures efficient amplitude transfer into the target excited state, while the nuclei evolve classically on the active potential energy surface as determined by the FSSH [57].

The integration of LCT into the surface-hopping framework yields two important advances. First, the spectral content of the control pulse adapts dynamically to the instantaneous electronic energy gap and transition dipole orientations sampled along each

classical trajectory, resulting in chirped fields that naturally follow the evolving electronic structure. Second, the laser field influences nuclear motion only indirectly—by inducing transitions between potential-energy surfaces—so that the resulting dynamics reflect the topography of the target PES rather than direct field-driven forces [60].

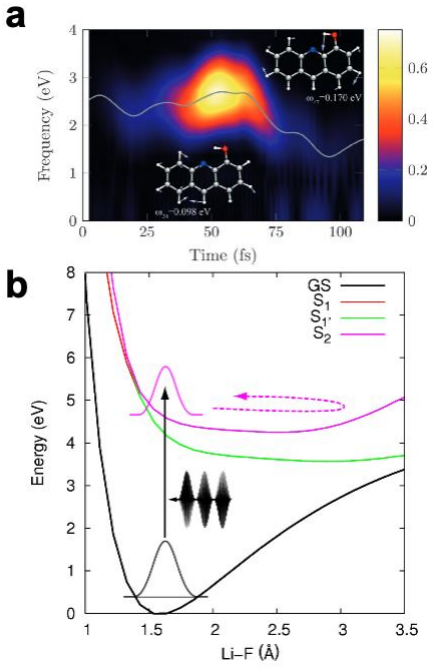

Figure 8. (a) Application of an LCT-optimized pulse spectrum to a poly-atomic chromophore, selectively exciting electronic states and modulating nonadiabatic population transfer. Adapted with permission from ref [60]. © *2015 WILEY-VCH Verlag GmbH & Co. KGaA, Weinheim*. Used with permission. (b) Pump control of Li-F, where the tailored pulse promotes selective excitation into higher-lying electronic states, thereby steering state-to-state dynamics along the dissociation coordinate. Adapted with permission from B. F. E. Curchod, T. J. Penfold, U. Rothlisberger, and I. Tavernelli, Phys. Rev. A 84, 042507 (2011). *Copyright (2011) by the American Physical Society*. https://doi.org/10.1103/PhysRevA.84.042507.

Representative applications highlight these principles. In proton-transfer chromophores, LCT/FSSH-generated fields selectively populated the S_1 state, thereby accelerating intramolecular proton transfer and revealing the cooperative role of high-frequency vibrations in promoting the reaction (**Figure 8a**) [60]. In contrast, for diatomic systems such as LiF, the same approach drives controlled excitation from the ground state to a bound excited state (S_2), achieving near-complete population transfer within a few hundred femtoseconds while producing pulses whose frequency content tracks the time-dependent energy gap (**Figure 8b**) [59]. These examples demonstrate how LCT, when embedded within an MQC dynamical framework, translates coherent-control concepts into a computationally tractable tool applicable to molecular systems of relevant size.

Collectively, these advances trace a coherent progression from quantum-dynamical demonstrations in model systems [42], to OCT/LCT-based pulse design in controlled dynamics [50,52–54], and finally to scalable MQC simulations in complex molecules [59,60]. By integrating rigorous control theories with computationally efficient dynamical methods, theory now offers both mechanistic insight into hidden intermediates and branching pathways, as well as predictive guidelines for designing experimentally realizable laser pulses [14,61].

Nevertheless, MQC approaches such as FSSH face three fundamental limitations that hinder their reliability in complex nonadiabatic processes. First, standard FSSH suffers from persistent electronic overcoherence, leading to inaccurate descriptions of decoherence and population branching. The surface hopping method incorporating the Nonadiabatic Field (NAF) mitigates these challenges by introducing a nonadiabatic nuclear force that drives independent trajectories, thereby enforcing physically consistent decoherence and branching during the dynamics [62]. The mapping approach to surface hopping (MASH) employs a Bloch-sphere–based continuous mapping representation for the electronic states, allowing them to evolve in a unified phase space and thereby addressing core deficiencies of FSSH, such as active-surface inconsistency, electronic overcoherence, and the violation of detailed balance [63]. Second, conventional FSSH completely neglects nuclear quantum effects—such as tunneling, zero-point motion, and quantum delocalization—that often play decisive roles in strongly anharmonic or barrier-crossing regions. Various nonadiabatic extensions of Ring-Polymer Molecular Dynamics (RPMD) [48,64–68] offer alternative routes to incorporate coherence and nuclear quantum effects beyond the limitations of standard FSSH. Finally, FSSH exhibits a strong dependence on the accuracy of the underlying electronic-structure calculations. Recent developments in high-precision machine-learning potential energy surfaces provide a promising route to alleviate this limitation by offering accurate energies and forces at a fraction of the computational cost [48,69–71].

3.3 Connection between theory and experiment

Despite significant conceptual advances in quantum-dynamical simulations and control-field design strategies, a substantial gap persists between theoretical predictions and experimental implementations of laser-controlled chemical reactions [72]. This disconnect arises from several interrelated challenges that span computational, molecular, and instrumental domains.

Computational and molecular-level challenges. Theoretical models often struggle to capture the full complexity of real molecular systems. Accurate simulations require computationally intensive multicoordinate calculations, which are substantially more demanding than traditional single-coordinate approaches. At the molecular level, designing systems with distinct, independently addressable reaction pathways—while ensuring vibrational decoupling and precise timing of control pulses—is critical to prevent rapid energy scrambling. In practice, control often relies on lower-frequency modes populated via high-frequency excitations, and metal centers can help localize vibrational energy to enhance selectivity [33,34].

Competing reaction channels and instrumental limitations. Upon photoexcitation, molecular systems frequently evolve along multiple strongly coupled reaction channels connected by conical intersections and non-adiabatic seams. This leads to rapid wave-packet bifurcation, making it difficult to selectively steer a single pathway [73]. Although theoretical schemes can identify field configurations that bias branching ratios toward a target outcome, experimental reproduction of this selectivity remains challenging due to the difficulty of suppressing competing channels.

Furthermore, while control theories often propose pulses with intricate temporal and spectral structures, experimental laser systems are constrained by limited bandwidth, achievable energy range, and phase stability. These hardware restrictions often reduce the transferability of theoretically optimized pulses to real-world experiments [74].

Environmental and system complexities. A major source of discrepancy arises from environmental effects. Experiments are typically conducted in condensed-phase environments (e.g., solutions or at interfaces), where solvent fluctuations, polarization effects, and energy dissipation significantly alter population dynamics and product distributions [75,76]. In contrast, most theoretical models assume isolated molecules or employ simplified Hamiltonians, leading to deviations between predicted and observed outcomes [76,77]. Bridging this gap requires not only advances in pulse-shaping technology, but also the development of more realistic theoretical frameworks that incorporate environmental interactions on an equal footing with electronic and nuclear dynamics.

Closing the theory-experiment gap in coherent control demands coordinated progress in three areas. First, more efficient and high-dimensional quantum dynamics simulations; second, molecular design strategies that enhance pathway-specific addressability; and third, experimental pulse-shaping technologies capable of delivering the complex field structures predicted by theory, particularly in realistic environments where decoherence and dissipation play decisive roles.

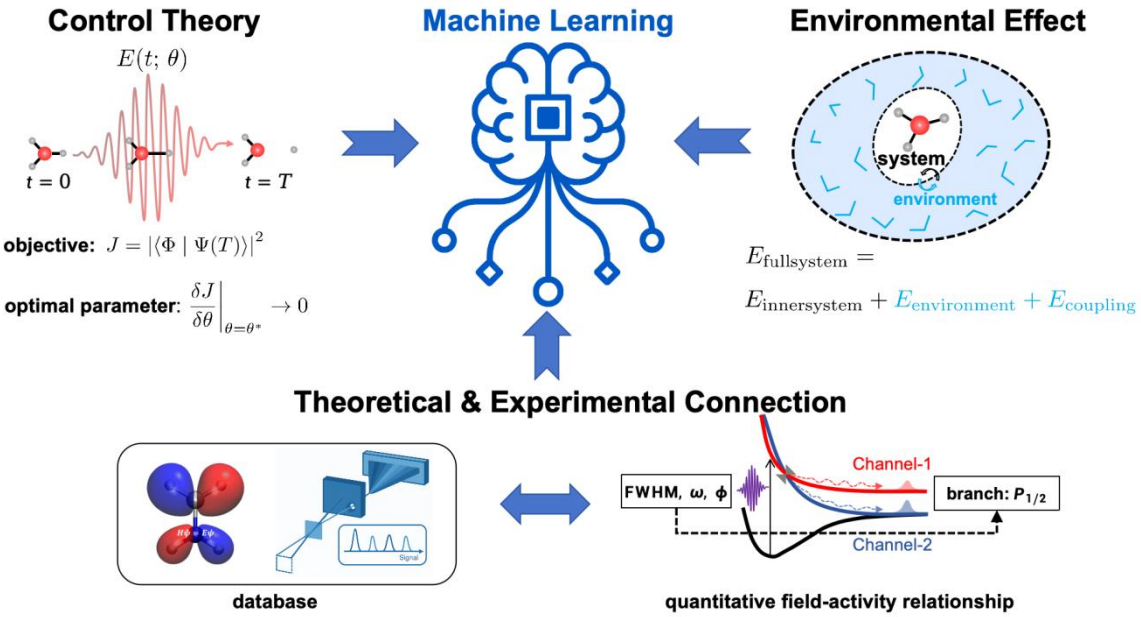

Figure 9. Machine learning serves as a pivotal integration layer, bridging theoretical simulations and experimental measurements: theoretical pulse design with experimental constraints (left), environmental modulation of reaction pathways (right), and hybrid data-driven predictive modeling (middle).

4. Perspective

In summary, significant progress on both theoretical and experimental fronts in field-controlled chemistry, however, several fundamental bottlenecks continue to constrain further advances. Key challenges include the experimental realizability of optimized laser pulses, limited channel selectivity within complex reaction spaces, and the pronounced influence of environmental factors on reaction pathways and yields. These limitations highlight the need for approaches that can integrate physical insight with scalable, data-driven strategies. To address these issues, we outline three prospective research directions empowered by machine learning (**Figure 9**). It has begun to provide practical tools for simulations relevant to optical-field-controlled chemistry. In particular, ML–potential energy surfaces have proven effective in excited-state simulations, including photodissociation dynamics and molecular-motor systems [48,69–71].

4.1 Control theory: toward experimentally feasible pulse design

Although control theories such as optimal control theory and local control theory can, in principle, generate optimized laser fields, the resulting pulses often exhibit intricate temporal and spectral structures that are analytically intractable and difficult to reproduce with current laser technology. To bridge this gap, future efforts should develop beyond-OCT/LCT frameworks that explicitly incorporate experimental constraints—such as bandwidth, dynamic range, and phase stability—into the optimization process. Machine learning can further support this direction by learning low-dimensional representations of OCT/LCT-optimized pulses. These learned representations can then be mapped onto experimentally realizable pulse families through hardware-aware surrogate models. Such approaches would yield pulse designs that are not only physically interpretable but also readily implementable, thereby enhancing the transferability of theoretical control schemes to experiments.

4.2 Toward environment-aware models via domain adaptation

Product distributions in realistic environments are strongly modulated by solvation, polarization, and interfacial conditions. However, most theoretical models are still limited to gas-phase or highly idealized settings, leading to significant extrapolation errors when comparing with condensed-phase experiments. To close this gap, future studies should develop environment-aware models that incorporate key solvent properties and interfacial fields. For the

critical challenge of transferring insights from gas-phase simulations to condensed-phase reality, ML-powered domain adaptation offers a solution. By learning environment-dependent corrections from hybrid datasets that blend simulation and experimental data, this strategy allows system-environment couplings to be quantified directly, enabling reliable predictions of reaction pathways and yields under realistic conditions. By learning system-environment couplings directly from data, such models can more accurately predict environment-dependent reaction pathways and yields. When calibrated with a limited set of experiments, domain adaptation techniques can further enhance the transferability of these models across diverse chemical environments, strengthening both predictive accuracy and experimental relevance.

4.3 Bridging theory and experiment in field-controlled reaction dynamics

External field excitation under realistic conditions often induces multichannel reaction dynamics with strong vibronic and solvent-mediated couplings. These interactions cause substantial wave-packet branching, which hinders selective control over reaction outcomes. Conventional electronic structure methods, such as density functional theory, frequently fail to capture strong electron correlation effects, while classical trajectory methods neglect essential nuclear quantum effects. As a result, simulating high-dimensional reaction spaces with quantitative accuracy remains challenging. A promising alternative is to combine accurate nonadiabatic trajectory simulations with limited experimental branching-ratio data to construct hybrid datasets. These can be used to train uncertainty-aware machine learning models that relate pulse parameters to channel-specific yields. When coupled with reinforcement learning, such models can efficiently identify pulse configurations that maximize desired products while explicitly accounting for environmental modulation.

In conclusion, while field-controlled chemistry faces significant challenges in transferring theoretical designs to experimentally viable applications—ranging from pulse realizability and limited channel selectivity to environmental interference—machine learning offers a unifying and adaptive framework to bridge these gaps. By integrating data-driven strategies across control theory, environmental modeling, and reaction dynamics, machine learning enables the development of interpretable, experimentally feasible pulse sequences. This machine learning-integrated framework charts a path toward controlling molecular processes in realistic environments, moving the field beyond gas-phase paradigms into functional materials and biological systems.

Acknowledgments

We appreciate support from the AI-Enhanced Research Program of Shanghai Municipal Education Commission (SMEC-AI-DHUY-06), Fundamental Research Funds for the Central Universities (2232023A-02), and National Natural Science Foundation of China (22422302, 12241407, 22173017).

References

[1] Ambartzumian R.V., Furzikov N.P., Gorokhov Yu.A., Letokhov V.S., Makarov G.N. and Puretzky A.A., Selective dissociation of sf6 molecules in a two-frequency infrared laser field. *Opt. Commun.,* **18** (4) (1976), 517–521.

[2] Letokhov V.S. and Moore C.B., Laser isotope separation (review). *Quantum Electron.,* **6** (2) (1976), 129–150.

[3] Brumer P. and Shapiro M., Control of unimolecular reactions using coherent light. *Chem. Phys. Lett.,* **126** (6) (1986), 541–546.

[4] Zewail A.H., Laser femtochemistry. *Science,* **242** (4886) (1988), 1645–1653.

[5] Merritt I.C.D., Jacquemin D. and Vacher M., Attochemistry: is controlling electrons the future of photochemistry? *J. Phys. Chem. Lett.,* **12** (34) (2021), 8404–8415.

[6] Hu D. and Huo P., Ab initio molecular cavity quantum electrodynamics simulations using machine learning models. *J. Chem. Theory Comput.,* **19** (8) (2023), 2353–2368.

[7] Hu D., Ying W. and Huo P., Resonance enhancement of vibrational polariton chemistry obtained from the mixed quantum-classical dynamics simulations. *J. Phys. Chem. Lett.,* **14** (49) (2023), 11208–11216.

[8] Roth M., Guyon L., Roslund J., Boutou V., Courvoisier F., Wolf J.-P. and Rabitz H., Quantum control of tightly competitive product channels. *Phys. Rev. Lett.,* **102** (25) (2009), 253001.

[9] Zhang Q., Zhu L., Zhou Z., Wang Z., Tian Y. and Liu Y., Dissociative photoionization studies of ethyl iodide using synchrotron radiation photoionization mass spectrometry and photoelectron imaging. *Chem. Phys. Lett.,* **817** (2023), 140427.

[10] Rabitz H. and Zhu W., Optimal control of molecular motion: design, implementation, and inversion. *Acc. Chem. Res.,* **33** (8) (2000), 572–578.

[11] Delor M., Sazanovich I.V., Towrie M. and Weinstein J.A., Probing and exploiting the interplay between nuclear and electronic motion in charge transfer processes. *Acc. Chem. Res.,* **48** (4) (2015), 1131–1139.

[12] Liebel M. and Kukura P., Lack of evidence for phase-only control of retinal photoisomerization in the strict one-photon limit. *Nat. Chem.,* **9** (1) (2017), 45–49.

[13] Solá I.R., González-Vázquez J., De Nalda R. and Bañares L., Strong field laser control of photochemistry. *Phys. Chem. Chem. Phys.,* **17** (20) (2015), 13183–13200.

[14] Brif C., Chakrabarti R. and Rabitz H., Control of quantum phenomena: past, present and future. *New J. Phys.,* **12** (7) (2010), 075008.

[15] Pathak S., Ibele L.M., Boll R., Callegari C., Demidovich A., Erk B., Feifel R., Forbes R., Di Fraia M., Giannessi L., Hansen C.S., Holland D.M.P., Ingle R.A., Mason R., Plekan O., Prince K.C., Rouzée A., Squibb R.J., Tross J., Ashfold M.N.R., Curchod B.F.E. and Rolles D., Tracking the ultraviolet-induced photochemistry of thiophenone during and after ultrafast ring opening. *Nat. Chem.,* **12** (9) (2020), 795–800.

[16] Vacher M., Boyer A., Loriot V., Lépine F. and Nandi S., Few-femtosecond isotope effect in polyatomic molecules

ionized by extreme ultraviolet attosecond pulse trains. *J. Phys. Chem. A,* **126** (34) (2022), 5692–5701.

[17] Dantus M. and Lozovoy V.V., Experimental coherent laser control of physicochemical processes. *Chem. Rev.,* **104** (4) (2004), 1813–1860.

[18] Wei Z., Li J., Zhang H., Lu Y., Yang M. and Loh Z.-H., Ultrafast dissociative ionization and large-amplitude vibrational wave packet dynamics of strong-field-ionized diiodomethane. *J. Chem. Phys.,* **151** (21) (2019), 214308.

[19] Ridente E., Hait D., Haugen E.A., Ross A.D., Neumark D.M., Head-Gordon M. and Leone S.R., Femtosecond symmetry breaking and coherent relaxation of methane cations via x-ray spectroscopy. *Science,* **380** (6646) (2023), 713–717.

[20] González-Vázquez J., García G.A., Chicharro D.V., Bañares L. and Poullain S.M., Evidencing an elusive conical intersection in the dissociative photoionization of methyl iodide. *Chem. Sci.,* **15** (9) (2024), 3203–3213.

[21] He L., Sun S., Lan P., He Y., Wang B., Wang P., Zhu X., Li L., Cao W., Lu P. and Lin C.D., Filming movies of attosecond charge migration in single molecules with high harmonic spectroscopy. *Nat. Commun.,* **13** (1) (2022), 4595.

[22] Han M., Ji J.-B., Blech A., Goetz R.E., Allison C., Greenman L., Koch C.P. and Wörner H.J., Attosecond control and measurement of chiral photoionization dynamics. *Nature,* **645** (2025), 95–100.

[23] Li M., Zhao L., Wang H., Li J., Wang W., Cai J., Hong X., Shi X., Zhang M., Zhao X., Weissenbilder R., Busto D., Gisselbrecht M., Ueda K., Luo S., Li Z. and Ding D., Attosecond spectroscopy reveals spontaneous symmetry breaking in molecular photoionization. *Sci. Adv.,* **11** (2025), eadw5415.

[24] Kobayashi Y., Chang K.F., Zeng T., Neumark D.M. and Leone S.R., Direct mapping of curve-crossing dynamics in ibr by attosecond transient absorption spectroscopy. *Science,* **365** (6448) (2019), 79–83.

[25] Zewail A.H., Femtochemistry: atomic-scale dynamics of the chemical bond using ultrafast lasers (nobel lecture). *Angew. Chem. Int. Ed.,* **39** (15) (2000), 2586–2631.

[26] Basnayake G., Hoerner P., Mignolet B., Lee M.K., Lin Y.F., Winney A.H., Debrah D.A., Popaj L., Shi X., Lee S.K., Schlegel H.B., Remacle F. and Li W., Ellipticity controlled dissociative double ionization of ethane by strong fields. *Phys. Chem. Chem. Phys.,* **23** (41) (2021), 23537–23543.

[27] Kaufman B., Rozgonyi T., Marquetand P. and Weinacht T., Coherent control of internal conversion in strong-field molecular ionization. *Phys. Rev. Lett.,* **125** (5) (2020), 053202.

[28] Mi Y., Wang E., Dube Z., Wang T., Naumov A.Y., Villeneuve D.M., Corkum P.B. and Staudte A., D_3^+ formation through photoionization of the molecular D_2–D_2 dimer. *Nat. Chem.,* **15** (9) (2023), 1224–1228.

[29] Corrales M.E., De Nalda R. and Bañares L., Strong laser field control of fragment spatial distributions from a photodissociation reaction. *Nat. Commun.,* **8** (1) (2017), 1345.

[30] Varvarezos L., Costello J.T., Long C., Achner J., Wagner R., Meyer M. and Grychtol P., Ionization–dissociation of methane in ultrashort 400 nm and 800 nm laser fields. *Chem. Phys. Lett.,* **775** (2021), 138687.

[31] Zhou L., Ni H., Jiang Z., Qiang J., Jiang W., Zhang W., Lu P., Wen J., Lin K., Zhu M., Dörner R. and Wu J., Ultrafast formation dynamics of D_3^+ from the light-driven bimolecular reaction of the D_2–D_2 dimer. *Nat. Chem.,* **15** (9) (2023), 1229–1235.

[32] Radziuk D. and Möhwald H., Ultrasonically treated liquid interfaces for progress in cleaning and separation processes. *Phys. Chem. Chem. Phys.,* **18** (1) (2016), 21–46.

[33] Delor M., Keane T., Scattergood P.A., Sazanovich I.V., Greetham G.M., Towrie M., Meijer A.J.H.M. and Weinstein J.A., On the mechanism of vibrational control of light-induced charge transfer in donor–bridge–acceptor assemblies. *Nat. Chem.,* **7** (9) (2015), 689–695.

[34] Delor M., Archer S.A., Keane T., Meijer A.J.H.M., Sazanovich I.V., Greetham G.M., Towrie M. and Weinstein J.A., Directing the path of light-induced electron transfer at a molecular fork using vibrational excitation. *Nat. Chem.,* **9** (11) (2017), 1099–1104.

[35] Paulus B.C., Adelman S.L., Jamula L.L. and McCusker J.K., Leveraging excited-state coherence for synthetic control of ultrafast dynamics. *Nature,* **582** (7811) (2020), 214–218.

[36] Hutchison C.D.M., Baxter J.M., Fitzpatrick A., Dorlhiac G., Fadini A., Perrett S., Maghlaoui K., Bodet Lefèvre S., Cordon-Preciado V., Ferreira J.L., Chukhutsina V.U., Garratt D., Barnard J., Galinis G., Glencross F., Morgan R.M., Stockton S., Taylor B., Yuan L., Romei M.G., Lin C.-Y., Marangos J.P., Schmidt M., Chatrchyan V., Buckup T., Morozov D., Park J., Park S., Eom I., Kim M., Jang D., Choi H., Hyun H., Park G., Nango E., Tanaka R., Owada S., Tono K., DePonte D.P., Carbajo S., Seaberg M., Aquila A., Boutet S., Barty A., Iwata S., Boxer S.G., Groenhof G. and Van Thor J.J., Optical control of ultrafast structural dynamics in a fluorescent protein. *Nat. Chem.,* **15** (11) (2023), 1607–1615.

[37] Rana A., Harville P.A., Khuu T. and Johnson M.A., Microcanonical kinetics of water-mediated proton transfer in microhydrated 4-aminobenzoic acid. *Science,* **389** (6765) (2025), 1143–1146.

[38] Jonas D.M., Two-dimensional femtosecond spectroscopy. *Annu. Rev. Phys. Chem.,* **54** (1) (2003), 425–463.

[39] Lozovoy V.V. and Dantus M., Laser control of physicochemical processes; experiments and applications. *Annu. Rep. Prog. Chem., Sect. C: Phys. Chem.,* **102** (2006), 227–258.

[40] Torosov B.T., Shore B.W. and Vitanov N.V., Coherent control techniques for two-state quantum systems: a comparative study. *Phys. Rev. A,* **103** (3) (2021), 033110.

[41] Yu Q. and Hammes-Schiffer S., Multidimensional quantum dynamical simulation of infrared spectra under polaritonic vibrational strong coupling. *J. Phys. Chem. Lett.,* **13** (48) (2022), 11253–11261.

[42] Tannor D.J., Kosloff R. and Rice S.A., Coherent pulse sequence induced control of selectivity of reactions: exact quantum mechanical calculations. *J. Chem. Phys.,* **85** (10) (1986), 5805–5820.

[43] Ohmori K., Wave-packet and coherent control dynamics. *Annu. Rev. Phys. Chem.,* **60** (1) (2009), 487–511.

[44] Geißler D., Marquetand P., González-Vázquez J., González L., Rozgonyi T. and Weinacht T., Control of nuclear dynamics with strong ultrashort laser pulses. *J. Phys. Chem. A,* **116** (46) (2012), 11434–11440.

[45] Hoki K., González L., Shibl M.F. and Fujimura Y., Sequential pump-dump control of photoisomerization

competing with photodissociation of optical isomers. *J. Phys. Chem. A,* **108** (31) (2004), 6455–6463.

[46] Kröner D. and Klaumünzer B., Laser-operated chiral molecular switch: quantum simulations for the controlled transformation between achiral and chiral atropisomers. *Phys. Chem. Chem. Phys.,* **9** (36) (2007), 5009–5017.

[47] Kröner D., Shibl M.F. and González L., Asymmetric laser excitation in chiral molecules: quantum simulations for a proposed experiment. *Chem. Phys. Lett.,* **372** (1–2) (2003), 242–248.

[48] Xu H., Zhu L., Yan F., Zhu M. and Wen J., Steering ultrafast photochemical reactions beyond the transition-state limit by tailored field. *ChemRxiv Preprint,* (2025)

[49] Sugawara M., Yoshizawa S. and Yabushita S., Coherent control of wavepacket dynamics by locally designed external field. *Chem. Phys. Lett.,* **350** (2001), 253–259.

[50] Umeda H., Takagi M., Yamada S., Koseki S. and Fujimura Y., Quantum control of molecular chirality: optical isomerization of difluorobenzo[c]phenanthrene. *J. Am. Chem. Soc.,* **124** (31) (2002), 9265–9271.

[51] Gräfe S., Marquetand P. and Engel V., Classical aspects emerging from local control of energy and particle transfer in molecules. *J. Photochem. Photobiol. A,* **180** (3) (2006), 271–276.

[52] Keefer D., Thallmair S., Matsika S. and De Vivie-Riedle R., Controlling photorelaxation in uracil with shaped laser pulses: a theoretical assessment. *J. Am. Chem. Soc.,* **139** (14) (2017), 5061–5066.

[53] Marquetand P. and Engel V., Analysis of laser fields for photoassociation and molecular stabilization derived from local control theory. *J. Phys. B: At. Mol. Opt. Phys.,* **41** (7) (2008), 074026.

[54] Yamaki M., Hoki K., Ohtsuki Y., Kono H. and Fujimura Y., Quantum control of a chiral molecular motor driven by laser pulses. *J. Am. Chem. Soc.,* **127** (20) (2005), 7300–7301.

[55] Crespo-Otero R. and Barbatti M., Recent advances and perspectives on nonadiabatic mixed quantum–classical dynamics. *Chem. Rev.,* **118** (15) (2018), 7026–7068.

[56] Curchod B.F.E. and Martínez T.J., Ab initio nonadiabatic quantum molecular dynamics. *Chem. Rev.,* **118** (7) (2018), 3305–3336.

[57] Tully J.C., Molecular dynamics with electronic transitions. *J. Chem. Phys.,* **93** (2) (1990), 1061–1071.

[58] Hammes-Schiffer S. and Tully J.C., Proton transfer in solution: molecular dynamics with quantum transitions. *J. Chem. Phys.,* **101** (6) (1994), 4657–4667.

[59] Curchod B.F.E., Penfold T.J., Rothlisberger U. and Tavernelli I., Local control theory in trajectory-based nonadiabatic dynamics. *Phys. Rev. A,* **84** (4) (2011), 042507.

[60] Curchod B.F.E., Penfold T.J., Rothlisberger U. and Tavernelli I., Local control theory in trajectory surface hopping dynamics applied to the excited-state proton transfer of 4-hydroxyacridine. *ChemPhysChem,* **16** (10) (2015), 2127–2133.

[61] Rabitz H., De Vivie-Riedle R., Motzkus M. and Kompa K., Whither the future of controlling quantum phenomena? *Science,* **288** (5467) (2000), 824–828.

[62] Wu B., He X. and Liu J., Nonadiabatic field on quantum phase space: a century after Ehrenfest. *J. Phys. Chem. Lett.,* **15** (2) (2024), 644–658.

[63] Richardson J.O., Lawrence J.E. and Mannouch J.R., Nonadiabatic dynamics with the mapping approach to surface hopping (MASH). *Annu. Rev. Phys. Chem.,* **76** (1) (2025), 663–687.

[64] Shakib F.A. and Huo P., Ring polymer surface hopping: incorporating nuclear quantum effects into nonadiabatic molecular dynamics simulations. *J. Phys. Chem. Lett.,* **8** (13) (2017), 3073–3080.

[65] Zhao R., You P. and Meng S., Ring polymer molecular dynamics with electronic transitions. *Phys. Rev. Lett.,* **130** (16) (2023), 166401.

[66] Richardson J.O. and Althorpe S.C., Ring-polymer molecular dynamics rate-theory in the deep-tunneling regime: connection with semiclassical instanton theory. *J. Chem. Phys.,* **131** (21) (2009), 214106.

[67] Limbu D.K. and Shakib F.A., Real-time dynamics and detailed balance in ring polymer surface hopping: the impact of frustrated hops. *J. Phys. Chem. Lett.,* **14** (38) (2023), 8658–8666.

[68] Liu X.-Y., Wang S.-R., Fang W.-H. and Cui G., Nuclear quantum effects on nonadiabatic dynamics of a green fluorescent protein chromophore analogue: ring-polymer surface-hopping simulation. *J. Chem. Theory Comput.,* **20** (9) (2024), 3426–3439.

[69] Xu H., Zhang B., Tao Y., Xu W., Hu B., Yan F. and Wen J., Ultrafast photocontrolled rotation in a molecular motor investigated by machine learning-based nonadiabatic dynamics simulations. *J. Phys. Chem. A,* **127** (37) (2023), 7682–7693.

[70] Li J. and Lopez S.A., Machine learning accelerated photodynamics simulations. *Chem. Phys. Rev.,* **4** (3) (2023), 031309.

[71] Muller C., Sršeň Š., Bachmair B., Crespo-Otero R., Li J., Mausenberger S., Pinheiro M., Worth G., Lopez S.A. and Westermayr J., Machine learning for nonadiabatic molecular dynamics: best practices and recent progress. *Chem. Sci.,* **16** (38) (2025), 17542–17567.

[72] Dey D. and Tiwari A.K., Controlling chemical reactions with laser pulses. *ACS Omega,* **5** (29) (2020), 17857–17867.

[73] Goswami D., Optical pulse shaping approaches to coherent control. *Phys. Rep.,* **374** (6) (2003), 385–481.

[74] Dugan M.A., Tull J.X. and Warren W.S., High-resolution acousto-optic shaping of unamplified and amplified femtosecond laser pulses. *J. Opt. Soc. Am. B,* **14** (9) (1997), 2348–2358.

[75] Venkatraman R.K. and Orr-Ewing A.J., Solvent effects on ultrafast photochemical pathways. *Acc. Chem. Res.,* **54** (23) (2021), 4383–4394.

[76] Van Der Walle P., Milder M.T.W., Kuipers L. and Herek J.L., Quantum control experiment reveals solvation-induced decoherence. *Proc. Natl. Acad. Sci. U.S.A.,* **106** (19) (2009), 7714–7717.

[77] Tiefenbacher M.X., Bachmair B., Chen C.G., Westermayr J., Marquetand P., Dietschreit J.C.B. and González L., Excited-state nonadiabatic dynamics in explicit solvent using machine learned interatomic potentials. *Digit. Discov.,* **4** (6) (2025), 1478–1491.